Breast Cancer Research and Treatment (2019) 177:77–91
https://doi.org/10.1007/s10549-019-05307-8

PRECLINICAL STUDY

Neuronatin is a modifier of estrogen receptor-positive breast cancer incidence and outcome

Cody Plasterer[1,2] · Shirng-Wern Tsaih[1,2] · Amy R. Peck[3] · Inna Chervoneva[4] · Caitlin O'Meara[1,2] · Yunguang Sun[3] · Angela Lemke[1,2] · Dana Murphy[1,2] · Jennifer Smith[1] · Sophia Ran[5,6] · Albert J. Kovatich[7] · Jeffrey A. Hooke[7] · Craig D. Shriver[7] · Hai Hu[8] · Edith P. Mitchell[9] · Carmen Bergom[10] · Amit Joshi[11] · Paul Auer[12] · Jeremy Prokop[13,14] · Hallgeir Rui[3] · Michael J. Flister[1,2]

Received: 15 November 2018 / Accepted: 29 May 2019 / Published online: 4 June 2019

Abstract

Purpose Understanding the molecular mediators of breast cancer survival is critical for accurate disease prognosis and improving therapies. Here, we identified Neuronatin (NNAT) as a novel antiproliferative modifier of estrogen receptor-alpha (ER+) breast cancer.

Experimental design Genomic regions harboring breast cancer modifiers were identified by congenic mapping in a rat model of carcinogen-induced mammary cancer. Tumors from susceptible and resistant congenics were analyzed by RNAseq to identify candidate genes. Candidates were prioritized by correlation with outcome, using a consensus of three breast cancer patient cohorts. NNAT was transgenically expressed in ER+ breast cancer lines (T47D and ZR75), followed by transcriptomic and phenotypic characterization.

Results We identified a region on rat chromosome 3 (142–178 Mb) that modified mammary tumor incidence. RNAseq of the mammary tumors narrowed the candidate list to three differentially expressed genes: NNAT, SLC35C2, and FAM210B. NNAT mRNA and protein also correlated with survival in human breast cancer patients. Quantitative immunohistochemistry of NNAT protein revealed an inverse correlation with survival in a univariate analysis of patients with invasive ER+ breast cancer (training cohort: $n=444$, HR = 0.62, $p=0.031$; validation cohort: $n=430$, HR = 0.48, $p=0.004$). NNAT also held up as an independent predictor of survival after multivariable adjustment (HR = 0.64, $p=0.038$). NNAT significantly reduced proliferation and migration of ER+ breast cancer cells, which coincided with altered expression of multiple related pathways.

Conclusions Collectively, these data implicate NNAT as a novel mediator of cell proliferation and migration, which correlates with decreased tumorigenic potential and prolonged patient survival.

Keywords Breast Cancer · NNAT · Cell cycle · Estrogen · Prognosis

Introduction

Breast cancer affects 1 in 8 women worldwide, resulting in 600,000 deaths annually [1–3]. In most cases, a single cause of breast cancer cannot be found, but rather multiple environmental and genetic factors contribute to overall disease susceptibility and outcome. This, combined with complex gene interaction in both malignant tumor cells and non-malignant tumor microenvironment cells, poses significant challenges in identifying new modifiers of breast cancer risk and outcome.

One strategy to identify breast cancer modifiers is through substitution of chromosomal regions of DNA (consomic) or subchromosomal regions of DNA (congenic) from inbred rodent strains with different susceptibility to mammary cancer. Adamovich et al. [4] used this approach to characterize mammary tumor risk in a panel of consomic rats that were constructed from the tumor-resistant BN strain and the tumor-susceptible SS rat strain. Following a single exposure to carcinogen, > 90% of SS rats developed mammary tumors by 15 weeks post-exposure, whereas the BN rats developed no macroscopically detectable mammary tumors. Substitution of the BN-derived rat chromosome 3 (RNO3) into the

✉ Michael J. Flister
mflister@mcw.edu

Extended author information available on the last page of the article

SS background (i.e., SS-3^{BN} consomic) significantly lowered mammary tumor incidence to < 30% ($p < 0.001$) and prolonged mean tumor latency ($p < 0.01$) compared with the SS parental strain [4]. Notably, this study did not resolve location of the genetic modifier(s) beyond the chromosomal level and the factor(s) on RNO3 that alter of mammary tumor risk remain unknown.

In this study, congenic mapping was used to localize a mammary tumor modifier region on RNO3 (142–178 Mb), which led to the discovery of Neuronatin (NNAT) as a novel antiproliferative suppressor of estrogen receptor-α positive (ER+) breast cancer. NNAT is a widely expressed proteolipid with numerous physiological and pathophysiological roles in neural development, metabolism, inflammation, and malignancy [5]. Although NNAT was previously linked to breast cancer, its functional role and impact on breast cancer incidence and outcome remains unclear. We provide the first consensus evidence that NNAT mRNA and protein correlate strongly with better overall survival (OS) and progression-free survival (PFS) in three large independent cohorts of patients with invasive breast cancer. Likewise, NNAT levels correlated with significantly lower mammary tumor incidence in response to carcinogen exposure in a syngeneic rat model, which coincided with decreased tumor cell proliferation. Phenotypic and transcriptomic analysis of two ER+ breast cancer cell lines revealed that NNAT suppresses tumor cell cycle, which potentially occurs through disruption of ER signaling. Collectively, these findings support that NNAT suppresses incidence and improves outcome of ER+ breast cancer.

Materials and methods

Generation of SS-3^{BN} consomic and congenic rats

All animal protocols were approved by the Institutional Animal Care and Use Committee of the Medical College of Wisconsin. The SS-Chr 3BN/Mcwi (SS-3^{BN}) consomic strain was generated by selectively breeding the SS/Mcwi (SS) and BN/Mcwi (BN) strains, as previously described [6]. Congenic strains were generated by crossing SS/Mcwi and the SS-3^{BN} consomic strain, followed by intercrossing the F1 progeny and F2 generation to capture different regions of RNO3 by marker-assisted selection, as described previously [7]. This approach resulted in four new congenic strains, which are described further in Fig. 1A.

Spontaneous mammary tumor model

Mammary tumors were induced by a single oral gavage of 7,12-dimethylbenz[a]anthracene (DMBA) in sesame seed oil (65 mg/kg) administered to female SS, SS-3^{BN}, line A, and line B rats at 49-55 days-of-age. Rats were palpated every week to record tumor incidence and latency. At 15 weeks, rats were euthanized and tumors were collected, weighed, and snap-frozen for further analysis.

Whole mount stain of mammary glands

Carmine alum staining of whole inguinal mammary glands was performed using standard protocols. Briefly, excised 4th and 5th mammary glands from left and right side of virgin female rats at 49–55 days-of-age were stretched and pressed onto a 2 × 3 inch glass slide and fixed 24 h in Carnoy's fixative. Following rehydration with H_2O, slides were stained in Carmine Alum stain 24 h and then serially dehydrated in ethanol. Finally, slides were cleared in Histo-Clear™ clearing reagent up to 72 h until transparent, and coverslipped using Histomount mounting media. Images were acquired on Nikon SMZ1500 Microscope.

Analysis of candidate gene expression in the TCGA-BRCA and KMplotter-BRCA cohorts and correlation with outcome

RNAseq data from 888 female breast cancer patients from the TCGA-BRCA cohort and the corresponding clinical parameter data were downloaded from the Broad GDAC Firehose (https://gdac.broadinstitute.org/) using the R package TCGA2STAT (http://www.liuzlab.org/TCGA2STAT/). The maximally selected rank statistics from the 'maxstat' R package (https://www.r-project.org/) was used to determine the optimal cutpoint for dichotomization (high vs. low) of expression values of the candidate genes (i.e., NNAT, SLC35C2, and FAM210B). The prognostic value of the resulting dichotomized NNAT mRNA expression was evaluated using the Log-rank test and Kaplan–Meier curves. A Cox proportional hazards model was used to evaluate the prognostic value of dichotomized NNAT mRNA expression with outcome. Using the abovementioned methods, the prognostic value of NNAT mRNA expression was also evaluated using the same cutpoint-driven dichotomization in the patient cohort divided into the ER+ subtype ($n = 700$) and ER− subtype ($n = 188$). Similarly, the KM Plotter tool (http://kmplot.com/analysis/) was used to assess the correlation of NNAT, SLC35C2, and FAM210B mRNA expression with outcome (overall survival and progression-free survival) in 3951 total breast cancer cases, as well as 3082 ER+ cases and 869 ER− cases. Individual case numbers used for low and high expression groups of FAM210B, NNAT, and SLC35C2 can be found on each figure (Figs. S2–S4).

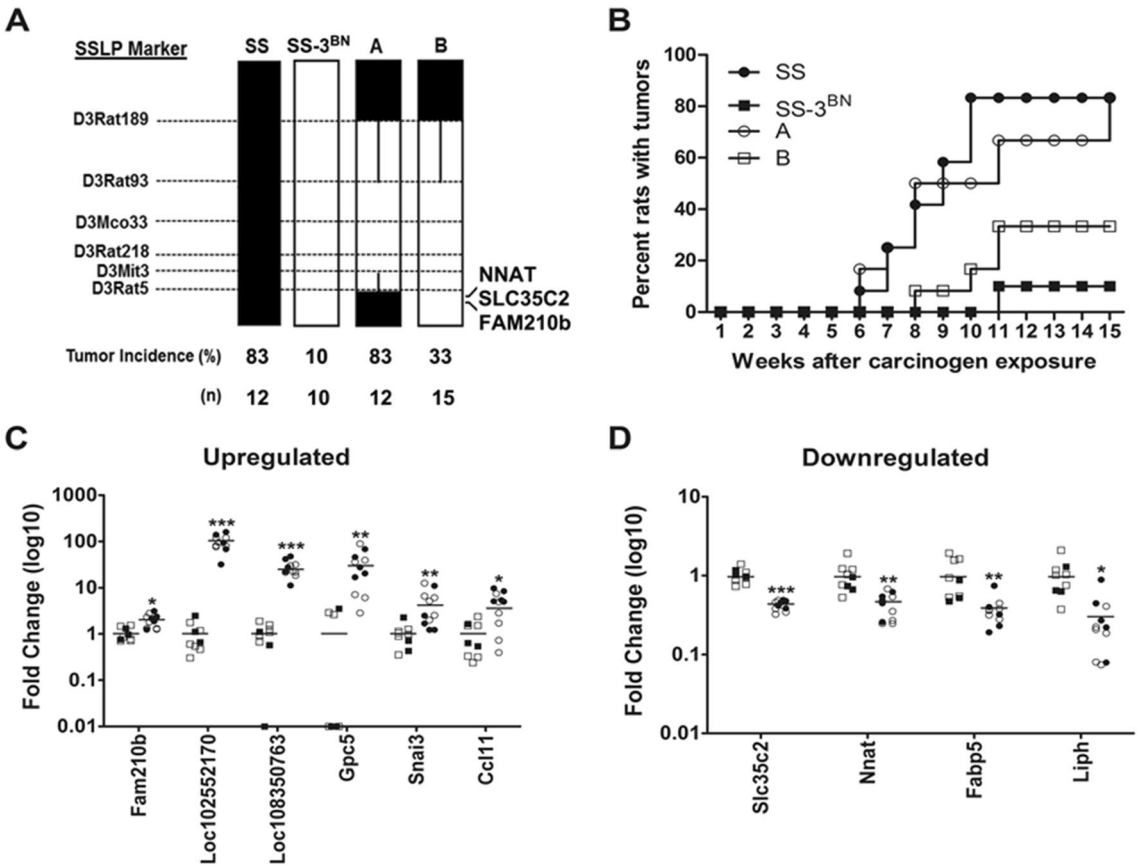

Fig. 1 **a** Congenic mapping localized a 36 Mb region on RNO3 (142–178 Mb) that modifies mammary tumor incidence. Schematic representation of SS-3^{BN} congenic strains that were generated by introgressing segments of BN chromosome 3 (black) into the genetic background of the parental SS strain (white) by marker-assisted breeding. Thin black bars represent confidence intervals, which are chromosomal regions that could be BN or SS. Following exposure to DMBA carcinogen, mammary tumor incidence and latency were recorded weekly for 15 weeks. **b** Tumor latency represented as the percentage of rats with mammary tumors at each time point. Closed circles = SS, open circles = line A, closed squares = SS-3^{BN}, open squares = line B. **c** Six genes that were differentially upregulated in expression within the RNO3 region (142–178 Mb) was detected by RNAseq analysis performed on tumors from rat strains with the SS-derived alleles within the region [SS ($n=5$) and line A ($n=6$)] compared with those that have the BN-derived alleles [SS-3^{BN} ($n=3$) and line B ($n=6$)]. (D) 4 genes that were differentially downregulated in expression within the RNO3 region (142–178 Mb) was detected by RNAseq analysis performed on tumors from rat strains with the SS-derived alleles within the region [SS ($n=5$) and line A ($n=6$)] compared with those that have the BN-derived alleles [SS-3^{BN} ($n=3$) and line B ($n=6$)]. $^{*}p<0.05$, $^{**}p<0.01$, $^{***}p<0.001$, as determined by Fisher's Exact Test (incidence), Log-Rank Test (latency), and FDR-corrected Student t test (RNAseq)

Quantitative immunofluorescent analysis of NNAT protein expression and its prognosis in patient with invasive breast cancer

A tissue bank of invasive breast cancer tissue specimens from 1988 to 2012 was collected into standard core-based tissue microarrays (TMAs) that were constructed using 0.6 mm core diameter (3DHistech Grandmaster). All immunohistochemistry, slide scanning, and quantitative analyses of digitized images were performed by investigators that were blinded to outcome. Immunohistochemistry for NNAT was performed on an autostainer (Omnis) using a previously validated rabbit anti-hNNAT antibody (1:400; ab27266, Abcam) [8], followed by linker and HRP-conjugated secondary antibody (Dako-Cat#K4003) and visualized using Cy5-tyramide as substrate, and multiplexed with anti-pan-cytokeratin antibody (mouse monoclonal, Dako-Cat#M3515) with Alexa555-labeled secondary antibody (Thermo-Fisher-Cat#A21422) to identify cancer cells, finalized by DAPI counterstain to visualize cell nuclei, as previously described [9–11]. Stained slides were scanned at ×20 magnification on a Scanscope laser scanner (Leica/Aperio) and fluorescent images were captured in three channels (Cy5-Alexa555-DAPI). Digitized images were analyzed by Tissue Studio (Definiens) and cytoplasmic expression signals for NNAT immunoreactivity were computed for individual cancer cells identified by pan-cytokeratin-positive mapping for each tumor core.

NNAT protein expression was computed as the median cytoplasmic cell signal intensity in the cancer cell population of each tumor.

Clinical outcome data (PFS) up to 240 months follow-up were available for 860 ER+ breast cancer patients, which were randomly divided into a training set ($n=433$; 79 recurrences) and a validation set ($n=427$; 60 recurrences) using a realization of the Bernoulli random variable with $p=0.5$. Recursive partitioning with tenfold cross-validation (rpart R package; http://www.R-project.org) was used to establish data-driven optimal cutpoints for dichotomization (high vs. low) of the NNAT expression. The prognostic value of the resulting dichotomized biomarker was evaluated in the validation set using the Log-rank test and Kaplan–Meier curves. The Cox proportional hazards model was used to evaluate the prognostic value of dichotomized NNAT expression univariately and multivariately, adjusting for important clinical-pathological prognostic factors. The initial multivariate Cox proportional hazards model included only known potential predictors of PFS: age, histology level (1, 2, or 3), node status, tumor size (< 2 cm, 2–5 cm, > 5 cm), dichotomized Ki67, radiation therapy indicator, chemotherapy indicator, and non-compliance with hormone therapy indicator. The parsimonious model was obtained using the backward elimination of non-significant covariates. Then dichotomized High vs. Low NNAT was added to this parsimonious model. The proportional hazard assumption was borderline significantly violated for metastases stage and, therefore, it was incorporated as a strata variable in the final Cox model.

Generation of transgenic ER+ breast cancer cell lines

T47D and ZR75 luminal B ER+ cell lines (originally obtained from ATCC) were transduced with lentivirus expressing NNAT (Origene, RC200328L3) or GFP (Origene, PS100071). All cell lines were mycoplasma-negative and were cultured for < 6 months. Transgene expression was confirmed by Western blotting, as described previously [12]. Briefly, cells were lysed in ice-cold buffer [50 mM tris (hydroxymethyl)aminomethane-HCl, pH 7.5, 150 mM NaCl, 1 mM ethylenediaminetetraacetic acid, 1% Triton-X100, 0.1% sodium dodecyl sulfate, phenylmethylsulphonyl fluoride 1:100, and protease inhibitor cocktail 1:50]. Proteins separated in a 4–20% sodium dodecyl sulfate–polyacrylamide gradient gel were transferred onto nitrocellulose membranes, followed by overnight incubation with primary antibodies against Flag-tag (Sigma, F3165) or β-actin (Abcam, ab6276). The next day, the membranes were washed and incubated for 1 h with horseradish peroxidase-conjugated secondary antibodies, followed by development with enhanced chemiluminescence reagent (Pierce).

Transwell migration assay

The migration of T47D and ZR75 transgenic cell lines was performed using 6-well transwell inserts (8 µm pore size; Corning). The cells were plated in triplicate into the upper chamber (1×10^6 cells/well) in RPMI-1640 (Gibco) containing 1% FBS. The bottom chambers were added with RPMI-1640 containing 10% FBS. 24 h post plating, non-migrated cells remaining on the upper surface of the membrane were removed using a cotton swab, and the migrated cells on the bottom surface were fixed with 2% paraformaldehyde, stained with 0.5% crystal violet, and photographed on a Nokia TS100 microscope. The numbers of migrated cells were counted in 4 randomly-selected fields and averaged for each chamber.

RNAseq analysis

Total RNA was extracted by Trizol from whole tumors that were excised from SS ($n=5$), line A ($n=6$), SS-3^{BN} ($n=3$), and line B ($n=6$), followed by library preparation using Illumina's TruSeq RNA library kit and sequencing on an Illumina HiSeq2500 (Illumina, Inc., San Diego, CA). The Trim Galore program (v0.4.1) was used to trim bases with a Phred quality score < 20 [https://www.bioinformatics.babraham.ac.uk/projects/trim_galore/] and only reads with a Phred quality score equal or higher than 20 were taken for analysis. The RSEM program function "rsem-prepare-reference" (v1.3.0) was used to extract the transcript sequences from the rat genome (build Rnor6.0) [13] and to generate Bowtie2 indices (Bowtie2 v2.2.8) [14], followed by read alignment using the "rsem-calculate-expression" function. Differential expression analysis was performed using the Bioconductor package DESeq2 version 1.12.4 [15] to compute log2 fold changes and false discovery rate-adjusted p values. Statistical significance was determined at a false discovery rate (FDR) threshold of 0.05.

RNAseq analysis was performed on ZR75 cells that transgenically expressed NNAT ($n=3$) or GFP ($n=3$; control). RNAseq libraries were constructed and analyzed as described above, with the exception of using the human genome (NCBI Build GRCh38.p2) for generation of the human transcriptome reference. Statistical significance of gene expression was determined as FDR < 0.05.

Single-cell RNAseq analysis

Values for 20 mouse organ single-cell datasets [16] were downloaded from https://figshare.com/articles/Single-cell_RNA-seq_data_from_Smart-seq2_sequencing_of_FACS_sorted_cells_v2_/5829687/7 and normalized to counts mapped for each gene per million counts mapped total. Nnat levels were extracted for average over all cells in each

tissue and for the percent of cells with > 10 Nnat mapped reads per million, designated as Nnat+. Values for all genes were extracted from the mammary gland cells and Log2 fold change calculated for genes found expressed in Nnat+ vs. Nnat− cells. The mouse cell atlas [17] was used to confirm subclustered mouse mammary gland biology using the MCA search tools (http://bis.zju.edu.cn/MCA/search.html).

Statistical analysis

All other statistical analyses were performed using Sigma Plot 11.0 software. Tumor incidence is defined as the percentage of rats that developed at least one tumor within each rat strain, presented as fraction of rats with and without tumors, which was analyzed by Fisher's Exact Test. Tumor latency is defined as the time (in weeks) it took for each strain to have 50% palpable tumors, presented as median weeks, analyzed by Pairwise Log-Rank Test. Data are presented as mean ± SEM. All data were analyzed by unpaired Student t test for two group comparisons or ANOVA for multi-group comparisons.

Results

Localization of a rat mammary tumor modifier region on RNO3

Modifier(s) of mammary tumorigenesis were previously detected on rat chromosome 3 (RNO3) using an SS-3^{BN} consomic strain [4, 6], prompting us to test whether the genetic modifier(s) of mammary tumorigenesis could be localized by congenic mapping. Mammary tumors were induced by a single carcinogenic exposure of age-matched female rats from the SS, SS-3^{BN} consomic, and SS-3^{BN} congenic rat strains (Fig. 1a). As previously reported [4], the mammary tumor incidence at 15 weeks was significantly reduced in the SS-3^{BN} consomic strain (10%; 1 out of 10 rats; $p < 0.01$) compared with the parental SS strain (83%; 10 out of 12 rats) (Fig. 1a). Of the congenic strains, the mammary tumor incidence in line A (83%; 8 out of 12 rats) was significantly higher than the SS-3^{BN} consomic ($p < 0.05$) and was indistinguishable from the SS strain (Fig. 1a). In contrast, mammary tumor incidence in line B (33%; 5 out of 15 rats) was significantly lower than in SS ($p < 0.05$) and was indistinguishable from the SS-3^{BN} consomic (Fig. 1a). Similarly, the latencies of mammary tumor incidence in SS-3^{BN} consomic (> 15 weeks) and line B (> 15 weeks) were significantly increased when compared with the SS (9 weeks; $p < 0.05$) and line A (10 weeks; $p < 0.05$) (Fig. 1b). No differences in mammary gland structures were observed immediately prior to carcinogen exposure (Fig. S1A–E), precluding the possibility that mammary gland development impacted tumor susceptibility [18, 19]. Thus, these data collectively demonstrate by exclusion mapping that a mammary tumor modifier region resides on rat chr3:142–178 Mb.

Genomic and transcriptomic analysis of the RNO3 candidate region

To begin prioritizing candidates within the RNO3 modifier region, analysis of SS/JrHsDMcwi and BN/NHsdMcwi genomes in the 36 Mb region (chr3:142–178 Mb) was conducted using the Rat Genome Database, RGSC Genome Assembly v6.0 (http://rgd.mcw.edu). Of the 45,144 total variants within the region, 32 SNPs were non-synonymous, of which eight were predicted to alter function of six unique proteins (Table S1). Four breast cancer GWAS loci have been identified within the human syntenic region of the RNO3 candidate interval (Table S2). However, none of eight SNPs that potentially alter protein function were in linkage disequilibrium ($r^2 < 0.8$) with the GWAS lead SNPs, suggesting that it is unlikely that these coding variants are the conserved mechanism(s) of breast cancer risk in human. RNAseq analysis was also performed on mammary tumors that arose from rat strains with the SS-derived alleles within the region [SS ($n = 5$) and line A ($n = 6$)] compared with those that have the BN-derived alleles [SS-3^{BN} ($n = 3$) and line B ($n = 6$)]. Of the coding variants, only AHCY, FAM83D, and LSM14B were expressed (> 10 normalized counts) in the mammary tumor tissues, yet none of the genomic candidates were differentially expressed between the groups (Table S3). Collectively, these data suggest that genetic variants that potentially alter protein function are unlikely to be the phenotypic drivers within the RNO3 candidate region.

In addition to coding variants, the RNAseq data were used to explore whether other candidates in the RNO3 candidate interval could be identified by differential expression between strains with the SS-derived alleles or BN-derived alleles within the region. This revealed ten genes that were differentially expressed between the SS/line A and SS-3^{BN}/line B groups (Fig. 1c, d and Table S3), of which NNAT, SLC35C2, and FAM210B were localized within the modifier region (chr3:142–178 Mb) (Fig. 1a). Collectively, the genomic and transcriptomic data preliminarily prioritized FAM210B, SLC35C2, and NNAT as potential modifiers of mammary tumorigenesis.

NNAT expression is correlated with improved survival of ER+ breast cancer patients

A consideration of the carcinogen-induced rat mammary tumors model is that they predominantly originate as luminal ER+ and rarely undergo distant metastasis [20, 21], which is the primary cause of breast cancer mortality [22]. Thus, to

test the translational impact of the differentially expressed candidates (FAM210B, SLC35C2, and NNAT) on breast cancer survival, the candidate genes were assessed for significant correlations with breast cancer outcome in two cohorts: TCGA-BRCA [23] and KMplotter [24] (Figs. S2–S4). Of the candidates, only the expression of NNAT mRNA was consistently significantly associated with breast cancer survival in both cohorts, regardless of OS or PFS: TCGA-BRCA (OS, HR = 0.59, $p = 0.006$) (Fig. S2A) and KMplotter-BRCA (PFS, HR = 0.75, $p < 0.001$; OS, HR = 0.77, $p = 0.025$) (Fig. S2B-C). NNAT expression also predicted better outcome in ER+ breast cancer patients of both cohorts: TCGA-BRCA-ER+ (OS, HR = 0.61, $p = 0.026$) (Fig. S2D) and KMplotter-BRCA-ER+ (PFS, HR = 0.82, $p = 0.026$; OS, HR = 0.72, $p = 0.067$) (Figs. S2E, F). NNAT expression was associated with outcome in the TCGA ER− breast cancer patients (OS, HR = 0.38, $p = 0.043$) (Fig. S2G) but not the KMplotter ER− breast cancer patients (PFS, HR = 0.79, $p = 0.061$; OS, HR = 0.74, $p = 0.28$) (Fig. S2H, I). The discrepancy between the two cohorts could be due to the limited number of ER- cases. Nonetheless, NNAT expression was progressively decreased in ER+ and ER− TCGA-BRCA tumors compared with normal control tissues ($p = 2.2 \times 10^{-16}$) (Fig. S5). Collectively, these data demonstrate that NNAT mRNA expression is downregulated in malignant tumors and correlates with significantly better outcome of ER+ breast cancer.

Only a single qualitative IHC analysis of NNAT protein expression and breast cancer outcome has been reported to date [8]. This moderately sized retrospective analysis ($n = 148$) reported that a higher immunoreactivity score (IRS) of NNAT protein correlated with worse PFS and overall survival [8], which is inconsistent with the survival analysis of NNAT mRNA (Fig. S2, S5). As such, we sought to re-examine the correlation of NNAT protein with breast cancer outcome, using a much larger cohort of ER+ breast cancer patients ($n = 874$ cases) (Table 1) and employing quantitative immunofluorescent imaging of NNAT protein expression using the same anti-NNAT antibody (ab27266, Abcam) [8]. In line with the previous findings [8], NNAT expression was predominantly colocalized with pan-CK^+ malignant breast epithelia (Fig. 2a–c) and was localized in the cytoplasm (Fig. 2d, e). However, in contrast to the previous report [8], NNAT protein expression on pan-CK^+ cancer cells was inversely correlated with PFS in univariate analysis of ER+ breast cancer, based on a training cohort (HR = 0.62, 95% CI 0.40–0.96; $p = 0.031$) and its confirmation in a validation cohort (HR = 0.48, 95% CI 0.29–0.79; $p = 0.004$) (Fig. 2f, g). Likewise, multivariable analysis, with the adjustment for other significant risk factors for disease recurrence, demonstrated that NNAT protein expression is an independent predictor of PFS in patients with invasive ER+ breast cancer (HR = 0.64, 95% CI 0.42–0.98; $p = 0.038$) (Table 2). Thus, despite the previous findings that worse breast cancer outcome correlated with increased NNAT protein detection by qualitative IRS analysis [8], quantitative immunofluorescent analysis of NNAT protein levels predicted better outcome in ER+ breast cancer, which is consistent with NNAT transcript association with outcome in the TCGA-BRCA and KMplotter-BRCA.

Table 1 Patient and tumor characteristics for study population

	N	%
All patients	860	
Recurred	139	16
White	707	82
Non-white	153	18
Grade 1	312	36
Grade 2	360	42
Grade 3	181	21
Unknown	7	1
Tumor size < 2 cm	513	60
Tumor size 2–5 cm	235	27
Tumor size > 5 cm	76	9
Unknown	36	4
Node negative	519	60
Node positive	293	34
Unknown	48	6
Distant mets = no	801	93
Distant mets = yes	26	3
Unknown	33	4
Ki67 negative	250	29
Ki67 positive	448	52
Unknown	162	19
Chemo = yes	361	42
Chemo = no	455	53
Unknown	44	5
Radiation = yes	377	44
Radiation = no	449	52
Unknown	34	4
Hormone Tx: done	186	22
Not indicated	180	21
Indicated, not done	229	27
Unknown	265	31

NNAT is expressed in the mammary gland and is correlated with estrogen signaling, proliferation, and migration

The abovementioned findings correlated NNAT expression with lower incidence of mammary tumorigenesis (Fig. 1) and better breast cancer patient outcome (Fig. 2), but did not establish a causative relationship between NNAT and the underlying mechanisms that likely contribute to malignant phenotypes in the mammary gland. To begin understanding the biological role of NNAT in the mammary gland,

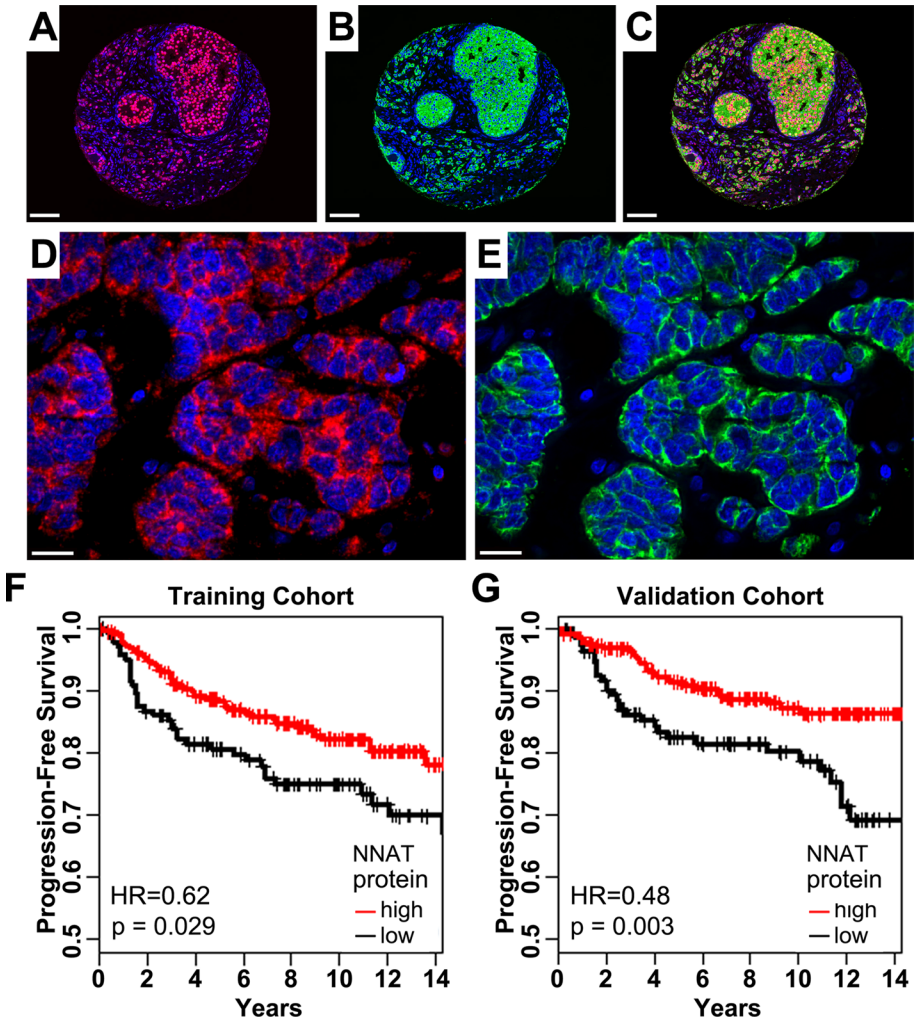

Fig. 2 NNAT immunostaining in ER+ breast cancer and Kaplan–Meier curves for progression-free survival by dichotomized NNAT protein expression. Immunofluorescent imaging of NNAT protein expression (red signal) that is colocalized to pan-CK+ tumor cells (green signal) at low resolution (**a–c**; × 12.9) and high resolution (**d, e**; × 60). Note the perinuclear localization of the NNAT within the cytoplasm of pan-CK+ malignant tumor cells (**d**). Scale bar represents 100 µm (**a**–**c**) and 20 µm (**d**, **e**). Median cancer cell immunofluorescence signal for NNAT protein was computed for each tumor in the training cohort and an objective data-driven cutpoint dichotomized tumors into Low NNAT (black line) and High NNAT (red line) expression which was used to obtain the Kaplan–Meier plot (**f**). The same cutpoint was then applied to generate a Kaplan–Meier plot for the Validation cohort (**g**). Censored cases are represented by hash marks on the plot lines

Table 2 Multiplicative hazard model in ER+ validation data set with dichotomized NNAT

Predictor	Hazard ratio	LL95%CI	UL95%CI	*p* value
Hormone Tx non-compliant	1.75	1.14	2.68	0.010
Histological grade 2 versus 1	1.38	0.82	2.35	0.228
Histological grade 3 versus 1	2.53	1.46	4.37	<0.001
Tumor size 2–5 cm versus < 2 cm	3.46	2.23	5.36	<0.001
Tumor size > 5 cm versus < 2 cm	3.61	1.94	6.72	<0.001
High versus low Ki67	1.60	1.03	2.48	0.035
High versus low neuronatin	0.64	0.42	0.98	0.038

we first examined the whole mouse single-cell RNAseq data generated by the Tabula Muris consortium [16]. Of the 20 normal tissues that were examined, the frequency of NNAT+ cells in the mammary gland (8% of total cells) was the third highest behind the brain (14%) and the pancreas (13%) (Fig. 3a). Using a second single-cell dataset of the Mouse Cell Atlas [17], we confirmed the clustering of *Nnat*+ cells in mammary gland involution (Fig. 3b), primarily in secretory alveoli and dendritic cells that are involved in cell apoptosis during weaning-induced involution [25]. A Spearman's correlation in NNAT+ cells was next used to assess the cellular physiological processes that correlate with NNAT expression in the mammary gland. Highly correlated genes (FDR < 0.1) with NNAT were significantly enriched in cell cycle regulatory pathways (IPA, $p = 3.81 \times 10^{-7}$; String-DB, FDR = 0.004) and cell motility pathways (IPA, $p = 5.90 \times 10^{-17}$, String-DB, FDR = 0.008) (Fig. 3c), both of which play key roles in mammary gland involution under normal physiological conditions and malignant transformation under pathophysiological conditions.

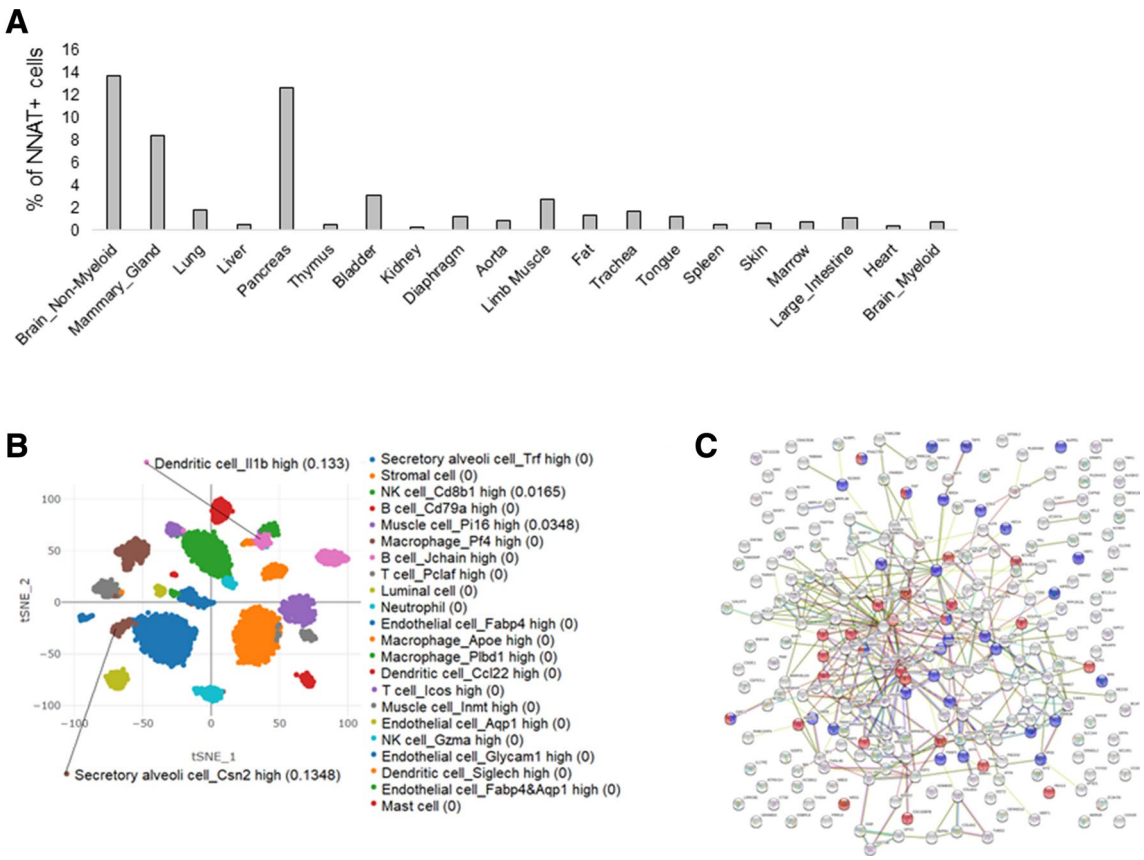

Fig. 3 Single-cell RNAseq analysis of NNAT expression in the mouse mammary gland. **a** Single-cell RNAseq data were downloaded from the Tabula Muris consortium to identify the organism-wide distribution of NNAT + cells in the mouse. **b** Single-cell RNAseq data from the mouse cell atlas revealed a subclustering of NNAT expression in mammary gland cells undergoing involution. **c** A Spearman's correlation of genes expressed with NNAT showed a significant enrichment of pathways involved in cell proliferation (blue dots) and motility (red dots)

Finally, the ER signaling pathway (IPA, $p = 1.21 \times 10^{-11}$) was the most significantly enriched molecular gene network that correlated with NNAT expression in the mammary gland, suggesting that NNAT potentially plays a key role in ER-dependent functions in normal mammary gland physiology and pathophysiology.

NNAT expression in ER+ breast cancer cells

To test the functional role of NNAT in malignant ER+ breast epithelial cells, NNAT or GFP (control) were transgenically expressed in the ER+ breast cancer cell lines, T47D and ZR75, followed by confirmation of Flag-tagged NNAT expression by Western blotting (Fig. 4a). RNAseq analysis of ZR75-GFP and ZR75-NNAT cells ($n = 3$ per group) was performed to assess the molecular gene networks that were altered by elevated NNAT expression. Compared with the ZR75-GFP control cells, a total of 2616 differentially expressed genes were detected in ZR75-NNAT cells (Table S4). Gene network analysis revealed multiple highly enriched gene networks (Fig. 4b), including ESR1 (ERα) signaling ($p = 3.9 \times 10^{-39}$; Fig. 4c; Table S5) and E2F1-regulated cell cycle ($p = 3.4 \times 10^{-14}$; Fig. 4d; Table S6). Notably, the E2F1-regulated cell cycle pathway was predicted to be significantly downregulated (Z score = -2.2) by elevated NNAT levels, which coincided with the significant downregulation of positive mediators of cell cycle (e.g., E2F1, E2F2, CCND1, CDK2, and CDK4) and upregulation of numerous suppressors of cell cycle (e.g., E2F7, CDKN1A, CDKN3, CDK2AP1, and CDKN2B) (Fig. 4e). Likewise, NNAT elevation induced high CDKN1A protein levels and a marked reduction in ERK1/2 phosphorylation (Fig. 4f) further demonstrating that NNAT suppresses cell cycle of ER+ breast cancer cells.

To directly assess whether NNAT expression modulates tumor cell proliferation, T47D and ZR75 cell lines that overexpressed NNAT or GFP (control) were seeded at low density and enumerated after 48 h. NNAT overexpression suppressed tumor cell proliferation in both ZR75 ($-43 \pm 5\%$, $p < 0.001$) and T47D ($-27 \pm 5\%$, $p < 0.001$)

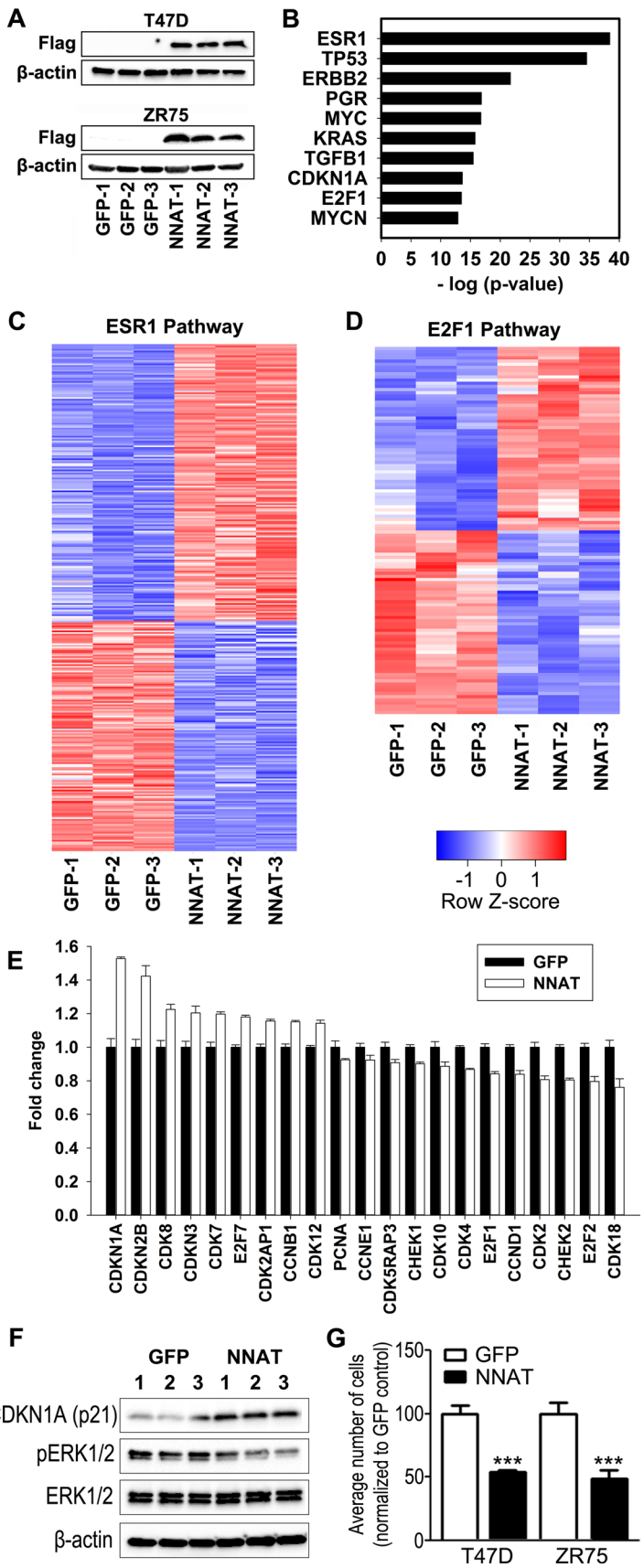

Fig. 4 RNAseq analysis of ER+ tumor cells following transgenic overexpression of NNAT or GFP in T47D and ZR75 cells ($n=3$ per group). **a** Transgenic overexpression of NNAT was confirmed by Western blot. **b** Gene network analysis revealed significant enrichment of the ESR1 (ERα) and E2F1 pathways. **c**, **d** Heatmaps of the enriched gene networks that re-associated with ESR1 (**c**) and E2F1 (**d**). **e** Bar graphs plots of the differential expression (FDR < 0.05) of key cell cycle mediators that are implicated in the ESR1 and E2F1 pathways. Data are presented as the mean fold expressions ± SEM ($n=3$ per group). **f** Western blotting of CDKN1A, phosphorylated ERK1/2, total ERK1/2, and β-actin ($n=3$ per group). **g** Proliferation of ER+ tumor cells following transgenic overexpression of NNAT or GFP in T47D and ZR75 cells. Data are presented as mean cell counts per well ± SEM ($n=18$ per group). ***$p<0.001$, as determined by Student t test

compared with the respective GFP controls (Fig. 4g). Likewise, positivity for the proliferative marker, phosphoHistone3 (PH3), was significantly higher in mammary tumors that arose in the rats with the lowly expressed SS-derived NNAT allele (23 ± 2 $PH3^+$ nuclei per field, $p < 0.001$) compared with mammary tumors that arose in the rats with the highly expressed BN-derived NNAT allele (9 ± 3 $PH3^+$ nuclei per field) (Fig. S6A–C).

In addition to sustained proliferative signaling, poor outcome of breast cancer patients has been attributed with increased cell survival and motility. To test whether NNAT altered cell survival, the ratio of caspase-3 to cleaved caspase-3 was assessed in T47D and ZR75 cells that overexpressed NNAT or GFP (control). Compared with the GFP control cells, no differences in the ratios of caspase-3 to cleaved caspase-3 were detected (Fig. S7). To evaluate if NNAT expression could impact tumor cell invasiveness, T47D and ZR75 cell lines that overexpressed NNAT or GFP (control) were seeded on transwell migration inserts for 24 h. NNAT overexpression suppressed tumor cell invasion in both ZR75 (8.78 ± 0.32 vs. 18.9 ± 0.66, $p < 0.001$) and T47D (12.6 ± 0.94 cells vs. 19.4 ± 1.50 cells per field, $p < 0.001$) (Fig. 5a–f). Likewise, the RNAseq analysis of ZR75 cells expressing GFP (control) or NNAT revealed a significant enrichment in cellular motility pathways ($p = 4.2 \times 10^{-32}$; Fig. 5g). Collectively, these data implicate NNAT as a novel suppressor of ER+ breast cancer by suppressing cancer proliferation and migration.

Discussion

The modifiers of breast cancer risk and outcome are complex in nature and remain poorly understood. Here, we used an unbiased mapping strategy to discover NNAT as a novel mediator of breast tumorigenesis (Fig. 1). Using multiple publically available datasets and the largest biomarker analysis of NNAT protein expression to date (Fig. 2, S2), we found that NNAT expression was significantly and independently correlated with better outcome in ER+ breast cancer. Gene network and phenotypic analysis of two ER+ breast cancer cell lines, T47D and ZR75, revealed that elevated NNAT altered the expression of gene networks linked with ER signaling, cell cycle, and cell motility, which coincided with significant inhibition of tumor cell proliferation and migration (Figs. 4, 5). Notably, many of the cell cycle regulatory genes that were altered by elevated NNAT levels were also downstream mediators of estrogen-stimulated proliferation [26], providing a potential mechanism by which NNAT suppresses ER+ breast cancer. Likewise, the ability of NNAT to suppress motility of ER+ breast cancer cells suggests another potential mechanism by which NNAT expression improves ER+ breast cancer patient survival.

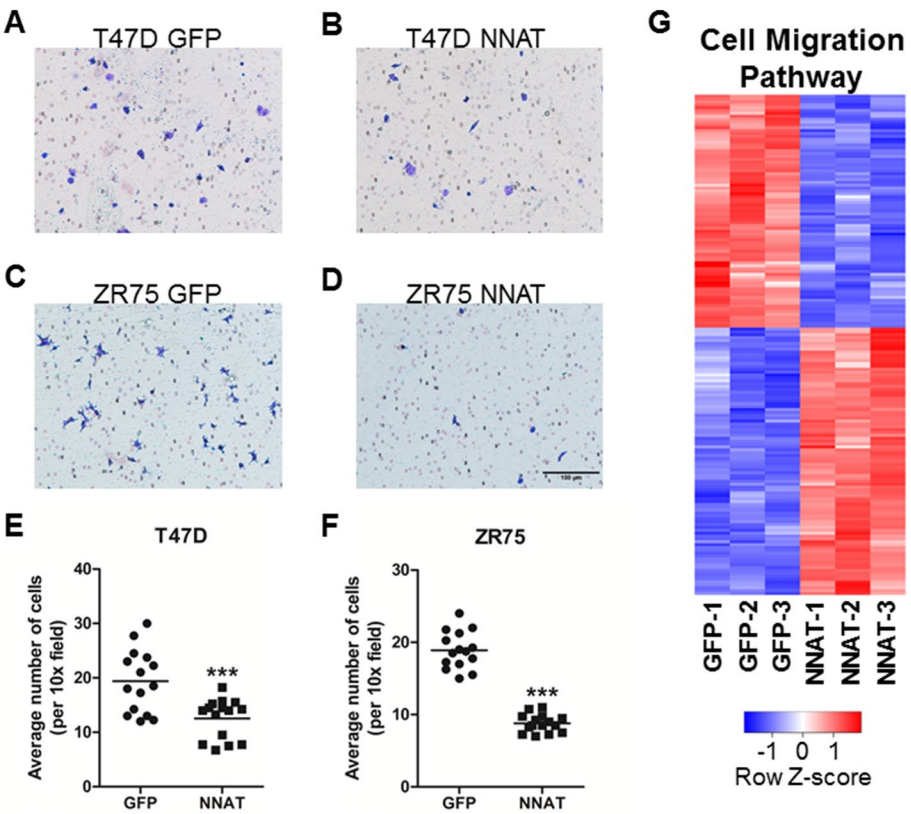

Fig. 5 NNAT overexpression inhibits the migration of ER+ breast cancer cell lines. **a** Representative image of T47D GFP cells on the bottom surface. **b** Representative image of T47D NNAT cells on the bottom surface. (**C**) Representative image of ZR75 GFP cells on the bottom surface. **d** Representative image of ZR75 NNAT cells on the bottom surface. **e** Average number of T47D GFP and T47D NNAT cells from 4 independent fields from 3 independent experiments. **f** Average number of ZR75 GFP and ZR75 NNAT cells from 4 independent fields from 3 independent experiments. **g** Gene network analysis revealed significant enrichment of the cell migration pathway. Date shown are individual chamber averages and the means of the data from at least 3 independent experiments ($n = 15$ wells/group). ***$p < 0.001$, as determined by Student *t* test

Collectively, these data strongly challenge the previously proposed role of NNAT as a predictor of worse outcome in breast cancer [8].

Evidence that NNAT is associated with improved patient outcome

Our data demonstrate that NNAT suppresses ER+ breast tumorigenesis and improves outcome, as demonstrated by the correlation of NNAT mRNA and protein with improved patient outcome in three large cohorts of invasive breast cancer. Additionally, we provide the first mechanistic evidence that NNAT expression inhibits tumor cell proliferation and motility, which has been widely correlated with improved breast cancer outcome in multiple studies. In contrast, the only other biomarker analysis of NNAT expression in breast cancer reported that the detection of abundant NNAT protein is associated with worse breast cancer outcome [8]. Reconciling these conflicting findings with the current study is challenging, due to the dramatic differences in cohort size (874 vs. 148 cases) and techniques (quantitative immunofluorescent analysis vs. qualitative IHC/IRS) that were used to evaluate the correlation of NNAT expression with breast cancer outcome. In contrast to the monochromatic DAB staining of NNAT protein in the previous study [8], we used dual-immunofluorescent imaging that enabled cell type-specific analysis of NNAT protein on CK+ cancer cells. Also, in contrast to the previous study using a single cohort of relatively small size [8], the current study used much larger test and validation cohorts to independently validate the inverse correlation of NNAT protein expression with ER+ breast cancer survival. Moreover, a multivariable analysis with the adjustment for other significant risk factors for recurrence demonstrated that NNAT protein expression independently predicted better outcome in patients with invasive ER+ breast cancer. One could argue that the technical advantages and greater statistical power of the current study strengthens the argument that NNAT suppresses breast cancer and improves ER+ breast cancer outcome, albeit future studies are warranted to further substantiate the role of NNAT in breast cancer.

Potential mechanistic role(s) of NNAT in ER+ breast cancer

NNAT is a widely expressed proteolipid with physiological and pathophysiological roles in neural development, metabolism, inflammation, and multiple malignancies [5]. NNAT is localized to the cytoplasm and endoplasmic reticulum in multiple cell types, including neurons [27, 28], adipocytes [29], and pancreatic beta cells [30], and regulates intracellular Ca^{2+} levels [28–31] through direct interaction with SERCA2 in the endoplasmic reticulum membrane [28]. Here, we presented the only experimental data exploring the baseline function(s) of NNAT in ER+ breast cancer, which revealed that NNAT markedly inhibits the proliferation of ER+ breast cancer cells in vitro and was inversely correlated with proliferative markers in vivo. Mechanistically, NNAT elevation in ER+ breast cancer cells altered the expression of numerous genes associated with ER signaling (315 genes; $p = 3.9 \times 10^{-39}$) and E2F1-regulated cell cycle (116 genes; $p = 3.4 \times 10^{-14}$), including upregulation of tumor suppressors (e.g., E2F7, CDKN1A, CDKN3, CDK2AP1, and CDKN2B) and downregulation of cell cycle mediators (e.g., E2F1, E2F2, CCND1, CDK2, and CDK4) [32].

ER signaling regulates the G_1/S phases of the cell cycle [26]. One of the most well-known growth-regulatory genes activated by ER signaling is Myc. Myc induces expression of cyclin D1 and Cdc25A. Cyclin D1 binds to cyclin-dependent kinase (Cdk4 or 6) which progresses the cell through the G_1 phase by activating cyclin E-Cdk2, hyperphosphorylation of pRb, activation of Cdc25A, and sequestering p21 [26]. ER signaling can increase cyclin D1 expression independent of Myc by activation of the cyclin D1 promoter via an estrogen response element [26]. Activation of cyclin E-Cdk2 complex, just like cyclin D1-Cdk4 or 6, leads to hyperphosphorylation of pRb and activation of Cdc25A [26]. Activation of Cdc25A is important for G_1 to S transition. Within the G_1 phase of the cell cycle is a restriction point. The way a cell passes the restriction point is through the hyperphosphorylation of pRb which then allows for the separation of the E2Fs which are bound to pRb. Of the E2F family, E2F1 and E2F2 promote the transition of the cell from G_1 to S plase by increasing the expression of Cdc25A and cyclin A [26].

Many of these steps in the G_1 and S phases are tightly regulated. All of the aforementioned cdks are regulated by cdk inhibitors, and are used to regulate the cell cycle. For example, p15, p21, and p57 can bind and block Cdk4 and Cdk6 activation, and p21 and p57 can bind and block cdk2 activation [26]. Cdk2 is also regulated by Doc1 [33], a subunit of the Anaphase-promoting complex (APC/C) which is an E3 ubiquitin ligase targeting proteins for degradation via the 26s proteasome. Although E2F1 is regulated by being bound to pRb, E2F7 can repress E2F1 target gene expression [34] (e.g., cyclin A), stopping the transition into S phase. Taken together, we hypothesize that overexpression of NNAT keeps the cells stuck in the G1/S transition of the cell cycle (Fig. 6).

It was recently established that the Cyclin D–Cdk4 signaling axis is a key driver of aggressive ER+ breast cancer [35–37], indicating that the novel observation of NNAT-mediated regulation of CCND1 (Cyclin D) and Cdk4 expression in ER+ breast cancer cells is clinically relevant. Moreover, Cdk4/6 inhibitors have quickly become a mainstream therapy for treating advanced ER+ breast cancer, yet no biomarkers for directing the use of Cdk4/6 inhibitors currently

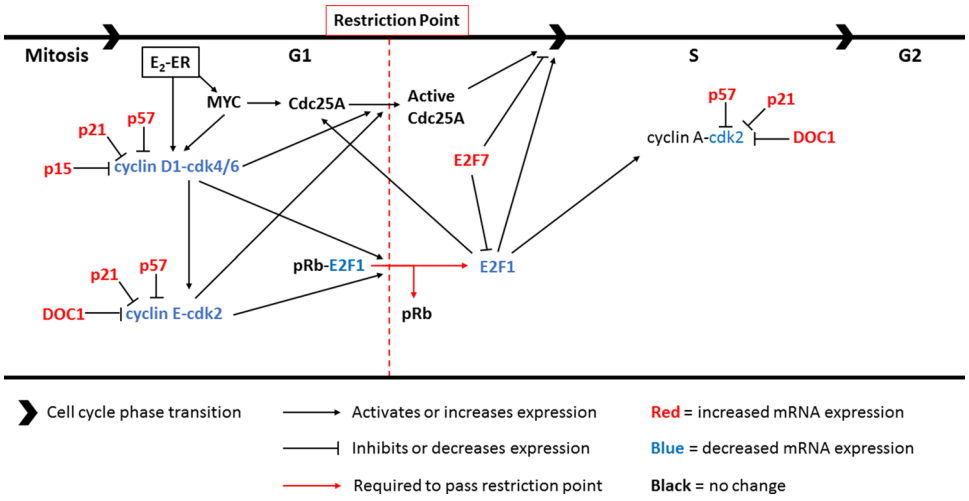

Fig. 6 Schematic of cell cycle regulators that were regulated by NNAT expression during the G_1-S phases of the cell cycle. The gene expression changes caused by transgenic overexpression of NNAT are denoted by red (increased mRNA expression), blue (decreased mRNA expression), or black (no change). Interactions that activate/increase expression, inhibit/decrease expression, or are required to pass the G_1 restriction point are indicated within the figure

exist [35]. Thus, based on our findings, future studies are now warranted to explore the mechanism(s) by which NNAT regulates cell cycle in ER+ breast cancer and to determine whether NNAT can be used as a novel biomarker for predicting therapeutic response to Cdk4/6 inhibitors.

A decrease in ER+ breast cancer motility caused by NNAT expression was also observed (Fig. 5), implicating another mechanism by which NNAT potentially improves outcome of ER+ breast cancer. Likewise, a significant enrichment of multiple pathways that regulate cell motility was observed in ZR75 cells overexpressing NNAT, including genes CITED2, LEPR, and OLR1 (Table S7). CITED2, interacts with several transcription factors, like the estrogen receptor, to enhance gene expression [38]. CITED2 has been found to facilitate breast cancer bone metastasis, and expression of CITED2 is inversely correlated with patient survival [38–40]. We observed a significant decrease in CITED2 expression when we overexpress NNAT in ZR75 cells (fold change = −0.806, $p < 0.001$, Table S3). The LEPR gene encodes the leptin receptor, which, when activated by leptin, signals the activation of pro-oncogenic pathways like JAK/STAT signaling [41]. In breast cancer, leptin receptor mRNA expression is positively correlated with cancer reoccurrence and mortality [42]. LEPR is significantly decreased in the ZR75 NNAT overexpression cells compared to the ZR75 GFP control cells (fold change = −0.754, $p < 0.001$, Table S3). OLR1 encodes the protein Lox1 which is the main receptor for oxidized LDL. OLR1 overexpression enhances migration of human breast cancer cells by activating NF-κB [43, 44], while depletion of OLR1 inhibits invasion and migration [45]. OLR1 is significantly downregulated in the ZR75 NNAT transgenic cell line compared to ZR75 GFP (fold change = −1.447, $p < 0.001$, Table S3). Future studies will be required to assess these and other potential downstream mechanisms that possibly mediate the role of NNAT in cell motility.

To our knowledge only one other study to date has examined the role of NNAT in cell migration and reported that NNAT overexpression increased migration of a single model of triple negative breast cancer (TNBC), MDA-MB-231 [31]. Reconciling these findings together with inhibitory role of NNAT in ER+ breast cancer migration is difficult due to only a single cell line of a different breast cancer subtype being examined in the only other in vitro breast cancer study to date. Thus, future studies are warranted to determine whether the NNAT-dependent effects on TNBC cell migration are limited to the single cell line that was analyzed (MDA-MB-231) or can be generalized to NNAT-dependent mechanism(s) that differentiate unique role(s) of NNAT in the TNBC and ER+ breast cancer subtypes.

Conclusions

Taken together, our data suggest that NNAT decreases incidence and improves ER+ breast cancer survival by suppressing tumor cell proliferation and motility. In addition to in vitro transcriptomic and phenotypic data, these conclusions were based on quantitative biomarker analyses in three large breast cancer cohorts, which challenged a prior qualitative analysis of NNAT protein expression in a much smaller cohort of breast cancer patients [8]. Reconciling this previous report with our current study is challenging due to the dramatic differences in technology and power between the two studies. However, we postulate that the strengths of the current study, including technical advantages (e.g., quantitative dual-immunofluorescent imaging) and greater statistical power (874 patients in two cross-validation cohorts), support the conclusion that NNAT is a suppressor of ER+ breast cancer. Likewise, mechanistic analyses of NNAT expression in ER+ breast cancer cell lines further substantiated the role of NNAT as novel regulator of cell cycle and

motility, which are widely implicated drivers of aggressive ER+ breast cancer [35–37]. Future studies will be necessary to further delineate the molecular interactions between NNAT, ER signaling, cell cycle, and motility, which contribute to therapeutic response and outcome of ER+ breast cancer.

Several other unanswered questions regarding the role(s) of NNAT in breast cancer risk and survival also remain to be addressed. Firstly, although our data suggest that NNAT is a phenotypic driver within the 36 Mb candidate region that is associated with rat tumorigenesis, it remains to be determined whether NNAT is the causative factor underlying the four GWAS loci that have been associated with breast cancer risk in the overlapping human syntenic region. Secondly, while our data suggest that NNAT is a regulator of ER+ breast cancer cell proliferation and motility, it has yet to be tested whether NNAT plays a role in other key aspects of patient survival, such as the metastatic cascade and resistance to anti-endocrine therapies. Nonetheless, at present, this study provides the first compelling evidence that NNAT is a novel modifier of ER+ breast cancer incidence and survival, potentially by suppressing cancer cell proliferation and motility.

Acknowledgements We thank Jozef Lazar for his assistance in generating the SS-3^{BN} congenic strains.

Funding This work was supported by a seed grant from the Wisconsin Breast Cancer Showhouse, the MCW Cancer Center, the Advancing a Healthier Wisconsin Endowment, and the Dr. Nancy Laning Sobczak Fund for Breast Cancer (M.J.F, H.R., C.B.). Support was also received from the NCI (R01CA193343 (M.J.F), R01CA188575 (H.R)); the Mary Kay Foundation (Grant No. 024-16 (M.J.F) and 017-29 (C.B.)); the METAvivor Foundation (M.J.F and H.R.); Susan G. Komen Grants KG091116 (H.R., E.P.M, I.C., A.J.K., C.D.S., J.A.H., and H.H.) and CCR17483233 (C.B), an American Cancer Society Institutional Research Grant (#86-004-26 (C.B.)); and the National Center for Research Resources, the National Center for Advancing Translational Sciences, and the Office of the Director of the NIH via the Clinical & Translational Science Institute (#8KL2TR000056 (C.B.)), NIH Office of the Director and NIEHS (K01ES025435 (J.W.P.)). The study was also supported by W81XWH-12-2-0050, HU0001-16-2-0004 from the U.S. Department of Defense through the Henry M. Jackson Foundation for the Advancement of Military Medicine (C.D.S., A.J.K., J.A.H., and H.H.). The views expressed in this article are those of the authors and do not reflect the official policy of the Department of the Army/Navy/Air Force, Department of Defense (DOD), or US Government.

Compliance with ethical standards

Conflict of interest The authors have no conflicts of interest to declare.

Ethical approval All applicable international, national, and institutional guidelines for the care and use of animals were followed. The Institutional Animal Care and Use Committee (IACUC) of the Medical College of Wisconsin approved all animal studies. All procedures involving animals were conducted in accordance with the National Institutes of Health guidelines concerning the use and care of experimental animals. All procedures performed in studies involving human participants were in accordance with the ethical standards of the institutional and/or national research committee and with the 1964 Helsinki declaration and its later amendments or comparable ethical standards. All histological breast cancer tissues were archival, de-identified specimens approved for use under waiver of consent by MCW IRB protocol PRO00028590.

Informed consent Informed consent was obtained from all individual participants included in the study.

References

1. Jemal A, Bray F, Center MM, Ferlay J, Ward E, Forman D (2011) Global cancer statistics. CA Cancer J Clin 61(2):69–90
2. Youlden DR, Cramb SM, Dunn NA, Muller JM, Pyke CM, Baade PD (2012) The descriptive epidemiology of female breast cancer: an international comparison of screening, incidence, survival and mortality. Cancer Epidemiol 36(3):237–248
3. Stewart BW, Wild C, International Agency for Research on Cancer, World Health Organization (2014) World cancer report 2014. WHO Press, Lyon
4. Adamovic T, McAllister D, Wang T, Adamovic D, Rowe JJ, Moreno C, Lazar J, Jacob HJ, Sugg SL (2010) Identification of novel carcinogen-mediated mammary tumor susceptibility loci in the rat using the chromosome substitution technique. Genes Chromosom Cancer 49(11):1035–1045
5. Pitale PM, Howse W, Gorbatyuk M (2017) Neuronatin protein in health and disease. J Cell Physiol 232(3):477–481
6. Flister MJ, Endres BT, Rudemiller N, Sarkis AB, Santarriaga S, Lemke A, Roy I, Geurts AM, Moreno C, Ran S et al (2014) CXM—a new tool for mapping breast cancer risk in the tumor microenvironment. Cancer Res. https://doi.org/10.1158/0008-5472.CAN-13-3212
7. Flister MJ, Tsaih SW, Stoddard A, Plasterer C, Jagtap J, Parchur AK, Sharma G, Prisco AR, Lemke A, Murphy D et al (2017) Host genetic modifiers of nonproductive angiogenesis inhibit breast cancer. Breast Cancer Res Treat 165(1):53–64
8. Nass N, Walter S, Jechorek D, Weissenborn C, Ignatov A, Haybaeck J, Sel S, Kalinski T (2017) High neuronatin (NNAT) expression is associated with poor outcome in breast cancer. Virchows Archiv 471(1):23–30
9. Peck AR, Witkiewicz AK, Liu C, Klimowicz AC, Stringer GA, Pequignot E, Freydin B, Yang N, Ertel A, Tran TH et al (2012) Low levels of Stat5a protein in breast cancer are associated with tumor progression and unfavorable clinical outcomes. Breast Cancer Res 14(5):R130
10. Sato T, Tran TH, Peck AR, Liu C, Ertel A, Lin J, Neilson LM, Rui H (2013) Global profiling of prolactin-modulated transcripts in breast cancer in vivo. Mol Cancer 12:59
11. Peck AR, Witkiewicz AK, Liu C, Stringer GA, Klimowicz AC, Pequignot E, Freydin B, Tran TH, Yang N, Rosenberg AL et al (2011) Loss of nuclear localized and tyrosine phosphorylated Stat5 in breast cancer predicts poor clinical outcome and increased risk of antiestrogen therapy failure. J Clin Oncol 29(18):2448–2458
12. Flister MJ, Wilber A, Hall KL, Iwata C, Miyazono K, Nisato RE, Pepper MS, Zawieja DC, Ran S (2010) Inflammation induces lymphangiogenesis through up-regulation of VEGFR-3 mediated by NF-kappaB and Prox1. Blood 115(2):418–429
13. Li B, Dewey CN (2011) RSEM: accurate transcript quantification from RNA-Seq data with or without a reference genome. BMC Bioinform 12:323

14. Langmead B, Salzberg SL (2012) Fast gapped-read alignment with Bowtie 2. Nat Methods 9(4):357–359
15. Love MI, Huber W, Anders S (2014) Moderated estimation of fold change and dispersion for RNA-seq data with DESeq2. Genome Biol 15(12):550
16. Tabula Muris C, Overall C, Logistical C, Organ C, Processing, Library P, Sequencing, Computational Data A, Cell Type A, Writing G et al (2018) Single-cell transcriptomics of 20 mouse organs creates a Tabula Muris. Nature 562(7727):367–372
17. Han X, Wang R, Zhou Y, Fei L, Sun H, Lai S, Saadatpour A, Zhou Z, Chen H, Ye F et al (2018) Mapping the mouse cell atlas by microwell-seq. Cell 172(5):1091–1107
18. Russo IH, Russo J (1996) Mammary gland neoplasia in long-term rodent studies. Environ Health Perspect 104(9):938–967
19. Russo J, Wilgus G, Russo IH (1979) Susceptibility of the mammary gland to carcinogenesis: I Differentiation of the mammary gland as determinant of tumor incidence and type of lesion. Am J Pathol 96(3):721–736
20. Shull J, Dennison K, Chack A, Trentham-Dietz A (2018) Rat models of 17beta-estradiol-induced mammary cancer reveal novel insights into breast cancer etiology and prevention. Physiol Genom 50(3):215–234
21. Russo J (2015) Significance of rat mammary tumors for human risk assessment. Toxicol Pathol 43(2):145–170
22. Ran S, Volk L, Hall K, Flister MJ (2010) Lymphangiogenesis and lymphatic metastasis in breast cancer. Pathophysiology 17(4):229–251
23. Cancer Genome Atlas N (2012) Comprehensive molecular portraits of human breast tumours. Nature 490(7418):61–70
24. Lanczky A, Nagy A, Bottai G, Munkacsy G, Szabo A, Santarpia L, Gyorffy B (2016) miRpower: a web-tool to validate survival-associated miRNAs utilizing expression data from 2178 breast cancer patients. Breast Cancer Res Treat 160(3):439–446
25. Akhtar N, Li W, Mironov A, Streuli CH (2016) Rac1 controls both the secretory function of the mammary gland and its remodeling for successive gestations. Dev Cell 38(5):522–535
26. Foster JS, Henley DC, Ahamed S, Wimalasena J (2001) Estrogens and cell-cycle regulation in breast cancer. Trends Endocrinol Metab 12(7):320–327
27. Lin HH, Bell E, Uwanogho D, Perfect LW, Noristani H, Bates TJ, Snetkov V, Price J, Sun YM (2010) Neuronatin promotes neural lineage in ESCs via Ca(2+) signaling. Stem Cells 28(11):1950–1960
28. Oyang EL, Davidson BC, Lee W, Poon MM (2011) Functional characterization of the dendritically localized mRNA neuronatin in hippocampal neurons. PLoS ONE 6(9):e24879
29. Suh YH, Kim WH, Moon C, Hong YH, Eun SY, Lim JH, Choi JS, Song J, Jung MH (2005) Ectopic expression of Neuronatin potentiates adipogenesis through enhanced phosphorylation of cAMP-response element-binding protein in 3T3-L1 cells. Biochem Biophys Res Commun 337(2):481–489
30. Joe MK, Lee HJ, Suh YH, Han KL, Lim JH, Song J, Seong JK, Jung MH (2008) Crucial roles of neuronatin in insulin secretion and high glucose-induced apoptosis in pancreatic beta-cells. Cell Signal 20(5):907–915
31. Ryu S, McDonnell K, Choi H, Gao D, Hahn M, Joshi N, Park SM, Catena R, Do Y, Brazin J et al (2013) Suppression of miRNA-708 by polycomb group promotes metastases by calcium-induced cell migration. Cancer Cell 23(1):63–76
32. Lim S, Kaldis P (2013) Cdks, cyclins and CKIs: roles beyond cell cycle regulation. Development 140(15):3079–3093
33. Wong T, Kim J, Khalid O, Sun H, Kim Y (2012) Double edge: CDK2AP1 in cell-cycle regulation and epigenetic regulation. J Dent Res 91(3):235–241
34. Carvajal L, Hamard P, Tonnessen C, Manfredi J (2012) E2F7, a novel target, is up-regulated by p53 and mediates DNA damage-dependent transcriptional repression. Genes Dev 26(14):1533–1545
35. O'Leary B, Finn RS, Turner NC (2016) Treating cancer with selective CDK4/6 inhibitors. Nat Rev Clin Oncol 13(7):417–430
36. Cristofanilli M, Turner NC, Bondarenko I, Ro J, Im SA, Masuda N, Colleoni M, DeMichele A, Loi S, Verma S et al (2016) Fulvestrant plus palbociclib versus fulvestrant plus placebo for treatment of hormone-receptor-positive, HER2-negative metastatic breast cancer that progressed on previous endocrine therapy (PALOMA-3): final analysis of the multicentre, double-blind, phase 3 randomised controlled trial. Lancet Oncol 17(4):425–439
37. Turner NC, Huang Bartlett C, Cristofanilli M (2015) Palbociclib in hormone-receptor-positive advanced breast cancer. N Engl J Med 373(17):1672–1673
38. Lau WM, Doucet M, Huang D, Weber KL, Kominsky SL (2013) CITED2 modulates estrogen receptor transcriptional activity in breast cancer cells. Biochem Biophys Res Commun 437(2):261–266
39. Lau WM, Weber KL, Doucet M, Chou YT, Brady K, Kowalski J, Tsai HL, Yang J, Kominsky SL (2010) Identification of prospective factors promoting osteotropism in breast cancer: a potential role for CITED2. Int J Cancer 126(4):876–884
40. Jayaraman S, Doucet M, Lau WM, Kominsky SL (2016) CITED2 modulates breast cancer metastatic ability through effects on IKKα. Mol Cancer Res 14(8):730–739
41. Myers MG Jr (2004) Leptin receptor signaling and the regulation of mammalian physiology. Recent Prog Horm Res 59:287–304
42. Sultana R, Kataki AC, Borthakur BB, Basumatary TK, Bose S (2017) Imbalance in leptin-adiponectin levels and leptin receptor expression as chief contributors to triple negative breast cancer progression in Northeast India. Gene 621:51–58
43. Khaidakov M, Mitra S, Kang BY, Wang X, Kadlubar S, Novelli G, Raj V, Winters M, Carter WC, Mehta JL (2011) Oxidized LDL receptor 1 (OLR1) as a possible link between obesity, dyslipidemia and cancer. PLoS ONE 6(5):e20277
44. Wang B, Zhao H, Zhao L, Zhang Y, Wan Q, Shen Y, Bu X, Wan M, Shen C (2017) Up-regulation of OLR1 expression by TBC1D3 through activation of TNFalpha/NF-kappaB pathway promotes the migration of human breast cancer cells. Cancer Lett 408:60–70
45. Hirsch HA, Iliopoulos D, Joshi A, Zhang Y, Jaeger SA, Bulyk M, Tsichlis PN, Liu XS, Struhl K (2010) A transcriptional signature and common gene networks link cancer with lipid metabolism and diverse human diseases. Cancer Cell 17(4):348–361

Affiliations

Cody Plasterer[1,2] · Shirng-Wern Tsaih[1,2] · Amy R. Peck[3] · Inna Chervoneva[4] · Caitlin O'Meara[1,2] · Yunguang Sun[3] · Angela Lemke[1,2] · Dana Murphy[1,2] · Jennifer Smith[1] · Sophia Ran[5,6] · Albert J. Kovatich[7] · Jeffrey A. Hooke[7] · Craig D. Shriver[7] · Hai Hu[8] · Edith P. Mitchell[9] · Carmen Bergom[10] · Amit Joshi[11] · Paul Auer[12] · Jeremy Prokop[13,14] · Hallgeir Rui[3] · Michael J. Flister[1,2]

1 Genomic Sciences and Precision Medicine Center, Medical College of Wisconsin, 8701 Watertown Plank Rd, Milwaukee, WI 53226, USA

2 Department of Physiology, Medical College of Wisconsin, Milwaukee, WI, USA

3 Department of Pathology, Medical College of Wisconsin, Milwaukee, WI, USA

4 Division of Biostatistics, Thomas Jefferson University, Philadelphia, PA, USA

5 Simmons Cancer Institute, Southern Illinois University School of Medicine, Springfield, IL, USA

6 Department of Medical Microbiology, Immunology, and Cell Biology, Southern Illinois University School of Medicine, Springfield, IL, USA

7 John P. Murtha Cancer Center, Uniformed Services University and Walter Reed National Military Medical Center, Bethesda, MD, USA

8 Chan Soon-Shiong Institute of Molecular Medicine at Windber, Windber, PA, USA

9 Medical Oncology, Thomas Jefferson University, Philadelphia, PA, USA

10 Department of Radiation Oncology, Medical College of Wisconsin, Milwaukee, WI, USA

11 Department of Radiology, Medical College of Wisconsin, Milwaukee, WI, USA

12 Joseph J. Zilber School of Public Health, University of Wisconsin-Milwaukee, Milwaukee, WI, USA

13 Department of Pediatrics and Human Development, College of Human Medicine, Michigan State University, Lansing, MI, USA

14 Department of Pharmacology and Toxicology, Michigan State University, East Lansing, MI, USA